ADVANCES IN ATMOSPHERIC SCIENCES, VOL. 23, NO. 1, 2006, 118–126

An Application of the Adjoint Method to a Statistical-Dynamical Tropical-Cyclone Prediction Model (SD–90) II: Real Tropical Cyclone Cases

XIANG Jie*[1,2] (项 杰), LIAO Qianfeng[1] (廖前锋), HUANG Sixun[1] (黄思训), LAN Weiren[1] (兰伟仁), FENG Qiang[3] (冯 强), and ZHOU Fengcai[4] (周凤才)

[1] *Institute of Meteorology, PLA University of Science and Engineering, Nanjing* 211101

[2] *Shanghai Institute of Typhoons, Shanghai* 200030

[3] *Institute of Atmospheric Physics, Chinese Academy of Sciences, Beijing* 100029

[4] *Shanghai Meteorological Center, Air Traffic Management Bereau of East China, Shanghai* 200066

(Received 25 February 2005; revised 16 November 2005)

ABSTRACT

In the first paper in this series, a variational data assimilation of ideal tropical cyclone (TC) tracks was performed for the statistical-dynamical prediction model SD–90 by the adjoint method, and a prediction of TC tracks was made with good accuracy for tracks containing no sharp turns. In the present paper, the cases of real TC tracks are studied. Due to the complexity of TC motion, attention is paid to the diagnostic research of TC motion. First, five TC tracks are studied. Using the data of each entire TC track, by the adjoint method, five TC tracks are fitted well, and the forces acting on the TCs are retrieved. For a given TC, the distribution of the resultant of the retrieved force and Coriolis force well matches the corresponding TC track, i.e., when a TC turns, the resultant of the retrieved force and Coriolis force acts as a centripetal force, which means that the TC indeed moves like a particle; in particular, for TC 9911, the clockwise looping motion is also fitted well. And the distribution of the resultant appears to be periodic in some cases. Then, the present method is carried out for a portion of the track data for TC 9804, which indicates that when the amount of data for a TC track is sufficient, the algorithm is stable. And finally, the same algorithm is implemented for TCs with a double-eyewall structure, namely Bilis (2000) and Winnie (1997), and the results prove the applicability of the algorithm to TCs with complicated mesoscale structures if the TC track data are obtained every three hours.

Key words: adjoint method, TC, double eyewalls, statistical-dynamical prediction model

1. Introduction

Tropical cyclone (TC) motion is one of the two core problems (tracks and intensity) in TC dynamics. In the early literature, a TC is usually regarded as a point vortex. Yeh (1950) and Kuo (1969), for instance, both viewed a TC as a point vortex (Rankine combined vortex) and studied TC motion and the impacts of the environment on TC motion. Their results indicated that TC motion often appears to be cyclonic trochoidal oscillations, the amplitudes and periods of which depend on the scale and intensity of the vortex and the displacement velocity of the ambient flow. Since the model of a point vortex is an oversimplified one, tracks of trochoidal oscillations can only describe part of the tracks of real TCs, and therefore, one gradually studies TCs from the vorticity viewpoint instead, which is now a prevailing concept in TC research. Based on the vorticity viewpoint, one largely understands the mechanism of TC motion using numerical simulation methods (Chan and Williams, 1987; Fiorino and Elsberry, 1987; Li and Zhu, 1990; Luo, 1991; Smith, 1991; Willoughby, 1992; Wu and Emanuel, 1993; Wu and Wang, 2000), and the prediction accuracy of TC tracks has improved greatly. This progress is summarized in Chan (2005). It is now acknowledged that

*E-mail: ahch65@yahoo.com.cn

the problem of predicting regular TC tracks has been solved. But for irregular TC tracks, such as those with sudden speedups, sudden slowdowns and even stagnation, sharp changes in direction, zig-zagging tracks, etc., there is not a powerful approach.

However, is the theory of a point vortex really incorrect? Perhaps it is not. For instance, the statistical-dynamical prediction model (SD) of TC tracks from the point vortex viewpoint developed by the Shanghai Institute of Typhoons is one of the successful operational models (Xue and Li, 1995), which has been updated from the earliest version SD-75 in the 1970s to SD-90 in the 1990s, and has a rather good accuracy for regular TC tracks. Besides, Xiang and Wu (2005) also established the relationship between TC motion and the asymmetric structures of the TC wind field, showing theoretically that the point vortex is a reasonable model.

In the first paper in this series (Xiang et al., 2004), the adjoint method was applied to SD-90 to study TC movements and ideal numerical tests were performed, and these showed that SD-90 has a good prediction ability. In the present paper, real TCs are considered, and the focus is centered on diagnostic aspects. Through the adjoint method, not only are real TC tracks fitted well, but also the forces acting on the TCs are retrieved.

This paper is laid out as follows. Section 2 covers the theoretical aspects; section 3 shows the application of the algorithm to real TC tracks with complete and partial TC track data; TCs with complicated mesoscale structures are considered in section 4; and the paper ends with conclusions and discussion in section 5.

2. The theoretical aspects

To help the render's understanding, the following presents the theoretical part of the application of the adjoint method to SD-90.

For SD-90, a TC is regarded as a point vortex whose motion satisfies

$$\begin{cases} \dfrac{dx}{dt} = u \ , \\ \dfrac{dy}{dt} = v \ , \\ \dfrac{du}{dt} = (f_0 + \beta y)v + F_x(t) \ , \\ \dfrac{dv}{dt} = -(f_0 + \beta y)u + F_y(t) \ , \\ x|_{t=0} = x_0 \ , \ \ y|_{t=0} = y_0 \ , \ \ u|_{t=0} = u_0 \ , \ \ v|_{t=0} = v_0 \ . \end{cases} \tag{1}$$

Here, $0 \leqslant t \leqslant T, (u, v)$ and (x, y) are the velocity and coordinates', respectively, of the TC center, and (F_x, F_y) is the force exerted on the TC excluding the Coriolis force $f_0 + \beta y$.

Suppose that over the interval $0 \leqslant t \leqslant T$, the observational TC track is $[X = X_{\rm obs}(t), Y = Y_{\rm obs}(t)]$. Now, the goal is to determine the optimal initial velocity (u_0, v_0) and forces $[F_x(t), F_y(t)]$, such that the corresponding solution $x(t), y(t), u(t), v(t)$ of Eq. (1) minimizes the functional

$$J[u_0, v_0, f_x(t), F_y(t)] = \frac{1}{2}\int_0^T \{[(x(t) - X_{\rm obs}(t)]^2 + [y(t) - Y_{\rm obs}(t)]^2\}dt \ . \tag{2}$$

It can be seen that the solution $u_0, v_0, f_x(t), f_y(t)$ is possibly not unique [in fact, it is an inverse problem to determine $u_0, v_0, f_x(t), f_y(t)$]. In order to obtain a unique physical solution, motivated by the thinking behind regularization, a stable functional is added to J so as to keep the solution unique, to speed up convergence of the solution, and to reduce numerical oscillations in the iterative process (Huang and Wu, 2001). In the meantime, motivated by the theory of optimal control, a terminal control term is also added to J so that the fitted track [namely $x(t), y(t)$] and the observational TC track [namely $X_{\rm obs}(t), Y_{\rm obs}(t)$] are kept as close as possible to each other at the terminal. Therefore, the new functional (still denoted by J)is

$$\begin{aligned} J[u_0, v_0, F_x(t), F_y(t)] = &\frac{1}{2}\int_0^T \{[x(t) - X_{\rm obs}(t)]^2 \\ &+ [y(t) - Y_{\rm obs}(t)]^2\}dt \\ &+ \frac{\gamma_1}{2}\int_0^T (u^2 + v^2)dt \\ &+ \frac{\gamma_2}{2}\int_0^T \left[\left(\frac{du}{dt}\right)^2 + \left(\frac{dv}{dt}\right)^2\right]dt \\ &+ \delta\{[x(T) - X_{\rm obs}(T)]^2 \\ &+ [y(T) - Y_{\rm obs}(T)]^2\} \ , \end{aligned} \tag{3}$$

where $\gamma_1, \gamma_2 > 0$ are referred to as the regularization parameters, and $\delta > 0$ is the restraint parameter at the terminal.

Assume that, for u_0, v_0 and $F_x(t), F_y(t)$, the solution of (1) is $x(t), y(t), u(t), v(t)$; for the disturbed $\tilde{u}_0 = u_0 + \alpha U, \tilde{v}_0 = v_0 + \alpha V$ (U, V are any fixed constants, α is an arbitrary constant) and the disturbed $F_x(t) + \alpha F_{1x}(t), F_y(t) + \alpha F_{1y}(t)$ [$F_{1x}(t), F_{1y}(t)$ are any fixed functions], the solution of Eq. (1) is $\tilde{x}(t), \tilde{y}(t), \tilde{u}(t), \tilde{v}(t)$. Define

$$\hat{s} = \lim_{\alpha \to 0} \frac{\tilde{s} - s}{\alpha} \ ,$$

where

$$s = x(t), y(t), u(t), v(t) \ .$$

Table 1. Main characteristics of five TCs.

TC	Occurrence	Initial position	Final position	Track direction
9112	2000 UTC 15 Aug–0200 UTC 25 Aug	21.1°N, 49.0°E	35.0°N, 120.5°E	Northwestward
9804	1400 UTC 25 AUg–1400 UTC 7 Sept	24.1°N, 132.9°E	48.1°N, 166.0°E	Northeastward
9908	2000 UTC 19 Aug–1400 UTC 23 Aug	16.9°N, 124.5°E	23.8°N, 112.8°E	Northwestward
9911	0800 UTC 16 Sept–0500 UTC 19 Sept	29.5°N, 128.1°E	32.0°N, 122.2°E	Westward to Northwestward North-
0115	1400 UTC 4 Sept–0800 UTC 12 Sept	18.7°N, 152.1°E	41.8°N, 145.7°E	westward turning to Northeastward

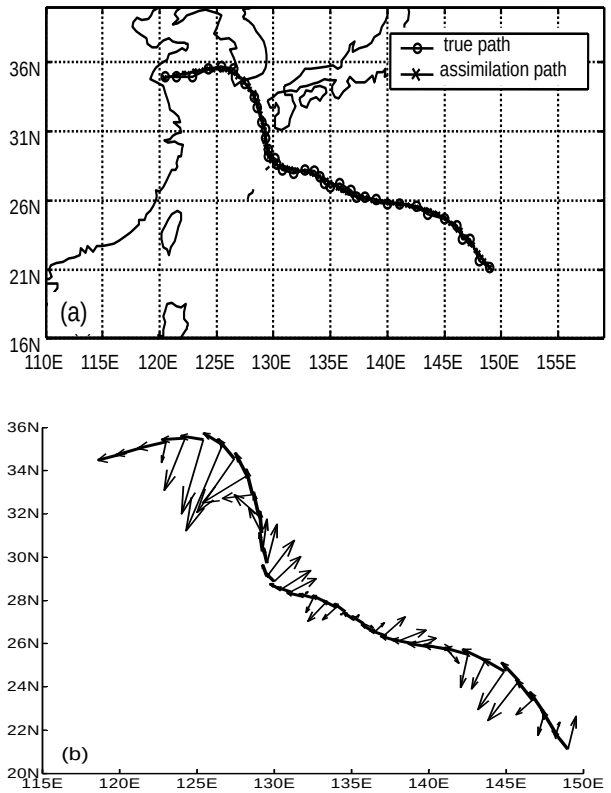

Fig. 1. TC 9112. (a) The fitted and real track; (b) The retrieved velocity vector (bold, unit: (°) h^{-1}) and the resultant of the retrieved force and Coriolis force (light, unit: ×116.8 N) during the whole span of the TC motion.

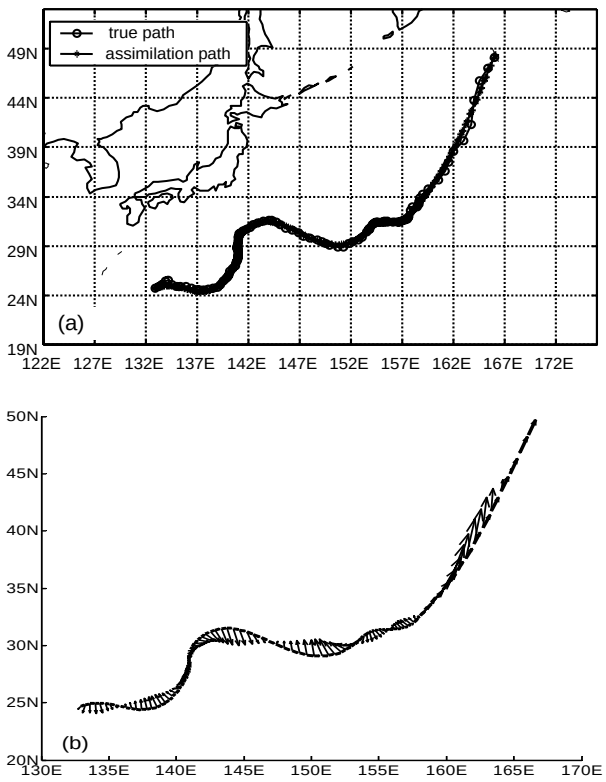

Fig. 2. TC 9804. (a) The fitted and real track; (b) The retrieved velocity vector (bold, unit: (°) h^{-1}) and the resultant of the retrieved force and Coriolis force (light, unit: ×116.8 N) during the whole span of the TC motion.

Then, the tangent linear model (TLM)of Eq. (1) is

$$\begin{cases} \dfrac{d\hat{x}}{dt} = \hat{u}\ , \\ \dfrac{d\hat{y}}{dt} = \hat{v}\ , \\ \dfrac{d\hat{u}}{dt} = (f_0+\beta y)\hat{v} + \beta v\hat{y} + F_{1x}\ , \\ \dfrac{d\hat{v}}{dt} = -(f_0+\beta y)\hat{u} - \beta u\hat{y} + F_{1y}\ , \\ \hat{x}|_{t=0} = 0,\ \ \hat{y}|_{t=0} = 0, \hat{u}|_{t=0} = U,\ \ \hat{v}|_{t=0} = V, \end{cases} \tag{4}$$

The adjoint equations and adjoint initial conditions are

$$\begin{cases} -\dfrac{dP}{dt} = x(t) - X_{\rm obs}\ , \\ -\dfrac{dQ}{dt} - \beta(vR - uS) = y(t) - Y_{\rm obs}\ , \\ -\dfrac{dR}{dt} - P + (f_0+\beta y)S = \gamma_1 u - \gamma_2 \dfrac{d^2u}{dt^2}\ , \\ -\dfrac{dS}{dt} - Q - (f_0+\beta y)R = \gamma_1 v - \gamma_2 \dfrac{d^2v}{dt^2}\ , \\ P(t) = \delta[x(T) - X_{\rm obs}(T)]\ , \\ Q(T) = \delta[y(T) - Y_{\rm obs}(T)]\ , \\ R(T) = \gamma_2 \dfrac{du}{dt}\Big|_{t=T}\ ,\ \ S(T) = \gamma_2 \dfrac{dv}{dt}\Big|_{t=T}\ . \end{cases} \tag{5}$$

Therefore the functional gradient of J at $[u_0, v_0, F_x(t),$

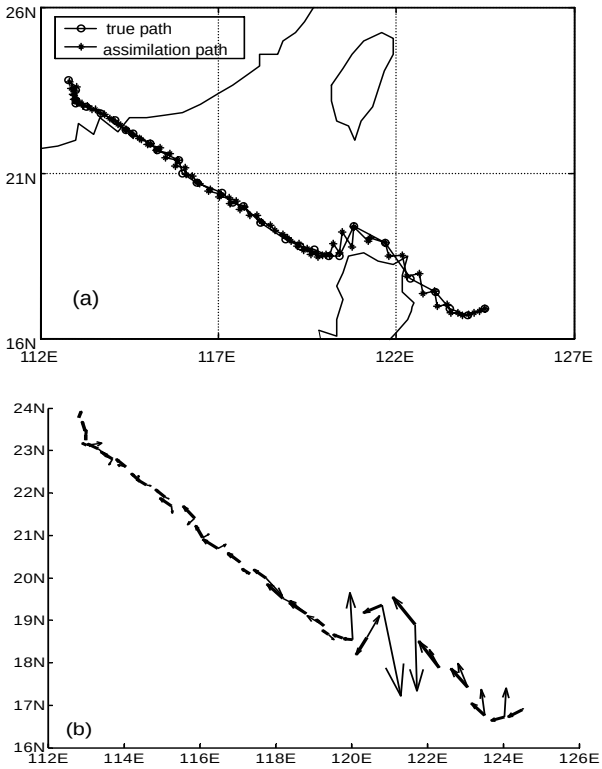

Fig. 3. TC 9908. (a) The fitted and real track; (b) The retrieved velocity vector (bold, unit: $(^\circ)\,\mathrm{h}^{-1}$) and the resultant of the retrieved force and Coriolis force (light, unit: $\times 116.8$ N) during the whole span of the TC motion.

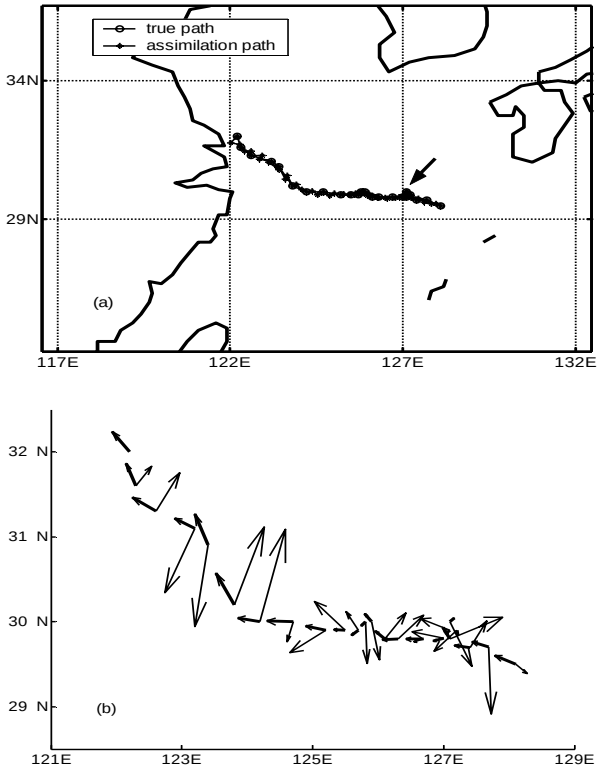

Fig. 4. TC 9911. (a) The fitted and real track, where the arrow indicates the portion of the track that is in a looping motion(see Fig. 6); (b) The retrieved velocity vector (bold, unit: $(^\circ)\,\mathrm{h}^{-1}$) and the resultant of the retrieved force and Coriolis force (light, unit: $\times 116.8$ N) during the whole span of the TC motion.

$F_y(t)]$ is

$$\begin{cases} \nabla_{u_0} J = R(0) - \gamma_2 \dfrac{du}{dt}\Big|_{t=0} , \\ \nabla_{v_0} J = S(0) - \gamma_2 \dfrac{dv}{dt}\Big|_{t=0} , \\ \nabla_{F_x} J = R(t), \ \ \nabla_{F_y} J = S(t) , \end{cases} \tag{6}$$

Setting $R = (R_1, R_2, R_3, R_4) = [u_0, v_0, F_x(t), F_y(t)]$, then, the descent algorithm can be expressed as follows

$$R_{j,i+1} = R_{j,i} + \nabla_{R_j} J|_{R_i} \cdot \rho_{j,i+1} . \tag{7}$$

3. Application to real TC tracks

In this section, five typical TC tracks occurring in the Northwest Pacific Ocean are chosen. These tracks are obtained through 3-hourly satellite positioning. By using the adjoint method, the initial velocity and forces exerted on the TCs are retrieved, and the tracks are fitted. The characteristics of five TCs are exhibited in Table 1.

In the following, the assimilation from complete track data is carried out first, and then the assimilation from incomplete track data is also done to verify the stability of the above algorithm.

3.1 *Assimilation from complete track data*

In the assimilations from complete track data for five typical TCs (9112, 9804, 9908, 9911, 0115), the real and the fitted tracks, as well as the relationship between the retrieved velocity vector and resultant of the retrieved forces and the Coriolis force, are shown in Figs. 1–5. Note that the assimilations fit the real tracks well.

It follows from Figs. 1–5 that the fitted tracks, retrieved velocities, and the resultants of the retrieved force and Coriolis force have the following properties:

(1) Although the TC motions are very complicated, the TC tracks can be fitted well, and the TC motions are analogous to those of particles. When the angle between the velocity and the resultant of the retrieved force and Coriolis force is small, or approaches 180 degrees, the TC tracks usually appear to be approximately straight lines, with the TC motion accelerating (small angle) or decelerating (the angle approaching 180 degrees). For example, for TCs 9804, 9908 and 0115, there exist portions of their tracks where the angle between the retrieved velocity and the resultant is small, and they move nearly straight.

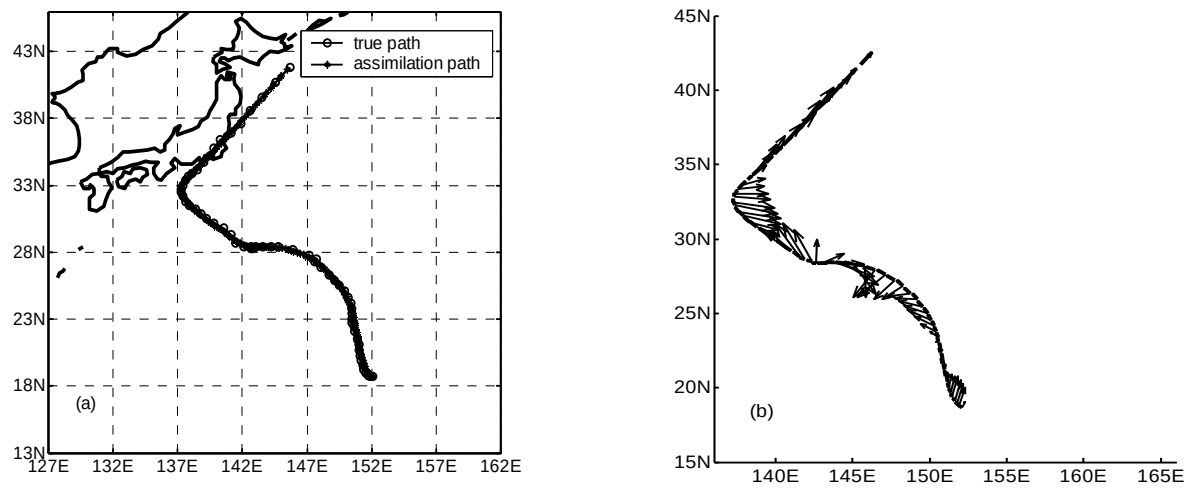

Fig. 5. TC 0115. (a) The fitted and real track; (b) The retrieved velocity vector (bold, unit: (°) h^{-1}) and the resultant of the retrieved force and Coriolis force (light, unit: ×116.8 N) during the whole span of the TC motion.

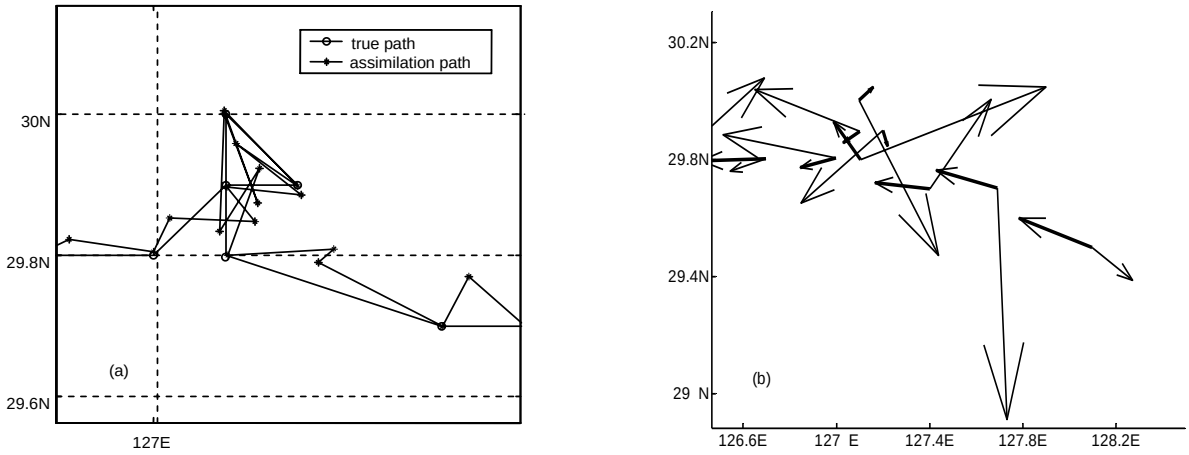

Fig. 6. Local magnification of Fig. 4. (a) Clockwise looping motion; (b) the corresponding retrieved velocity (bold, unit: (°) h^{-1}) and the resultant of the retrieved force and Coriolis force (light, unit: ×116.8 N).

(2) When the angle between the velocity and resultant is large, 90° or so, say, and the magnitude of the resultant is not small (if small, the turning is mostly slight), the TC tracks are curved, meaning that the TCs are turning sharply. This case occurs in all the above five TCs. In particular, for TC9911, there is a looping motion (marked by an arrow in Fig. 4a, see Fig. 6 below), which, along with the corresponding retrieved velocity vector and resultant in Fig. 4b, is magnified in Fig. 6. From Fig. 6, it can be seen that the third to seventh arrows (velocity vector) form a circuit, which means that the simulated TC motion is a looping one. When the magnitudes of the resultants vary from large to small, it seems that there are transition processes, meaning that tracks switch their convexity. This is especially clear for TCs 9112, 9804, and 0115.

(3) It seems that, in some cases, the resultants of the retrieved forces and Coriolis forces are distributed periodically (figures omitted here), which probably determines the periodicity of the TC tracks.

3.2 *Assimilation from incomplete track data*

In the above, the assimilation from complete track data of five typical TCs was performed, and the TC tracks were fitted well, and the forces were retrieved. These results indicate that the retrieved velocity and the resultant of the retrieved force and the Coriolis force match the fitted tracks well, and the TCs display particle-like motion. Because this algorithm depends on the observational data of TC tracks, an assimilation from incomplete track data is performed below to check the stability of this algorithm, using the track

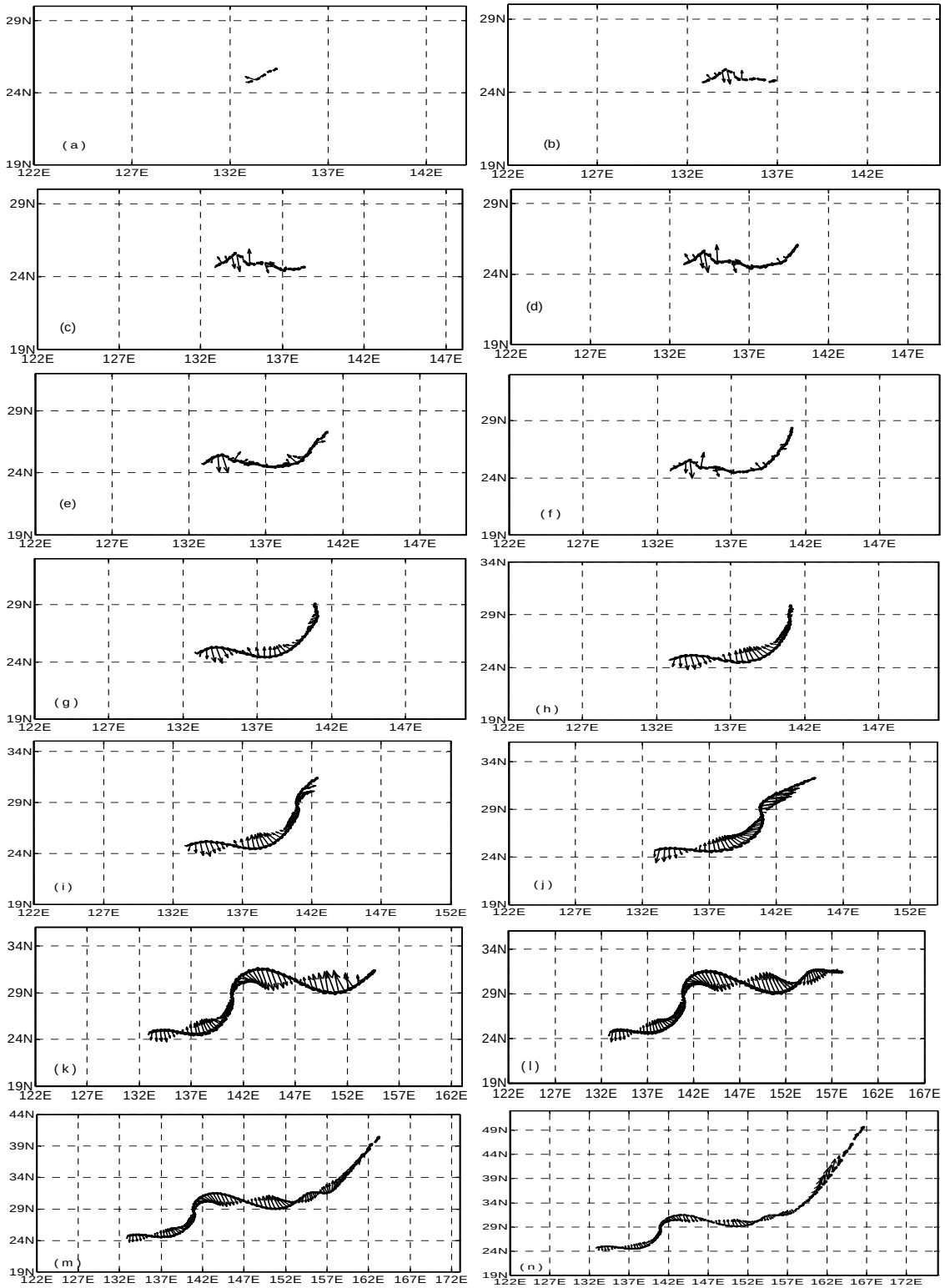

Fig. 7. The distribution of the retrieved velocity (bold, unit: $(^\circ)\,\mathrm{h}^{-1}$) and the resultant of the retrieved force and Coriolis force (light, unit: $\times 116.8$ N) for a portion of the TC 9804 track. (a) 12 hours; (b) 24 hours; (c) 36 hours; (d) 48 hours; (e) 60 hours; (f) 72 hours; (g) 84 hours; (h) 96 hours; (i) 108 hours; (j) 120 hours; (k) 168 hours; (l) 204 hours; (m) 240 hours; (n) 252 hours.

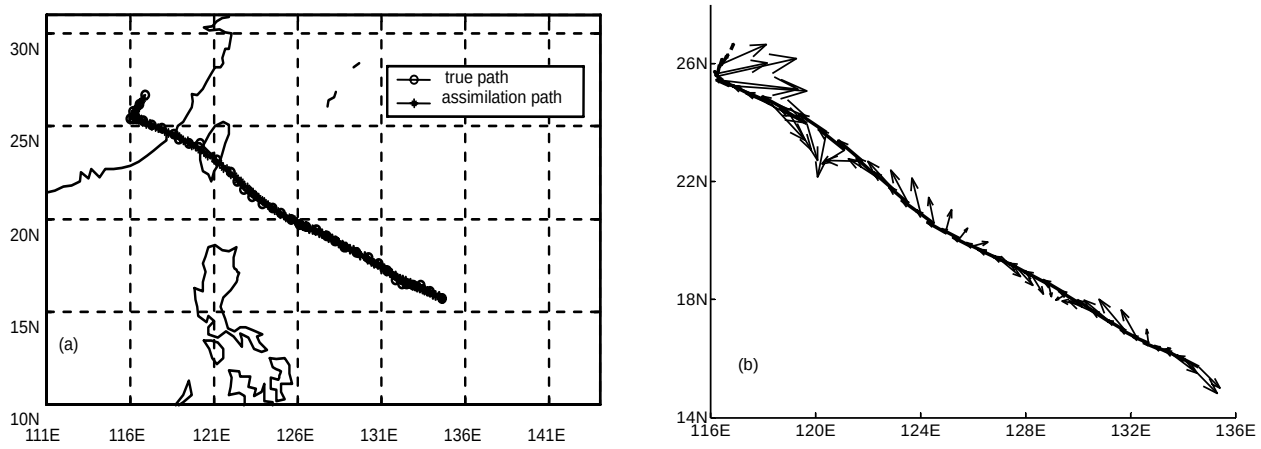

Fig. 8. TC Bilis. (a) The fitted and real track; (b) The retrieved velocity vector (bold, unit: (°) h^{-1}) and the resultant of the retrieved force and Coriolis force (light, unit: ×116.8 N) during the whole span of the TC motion.

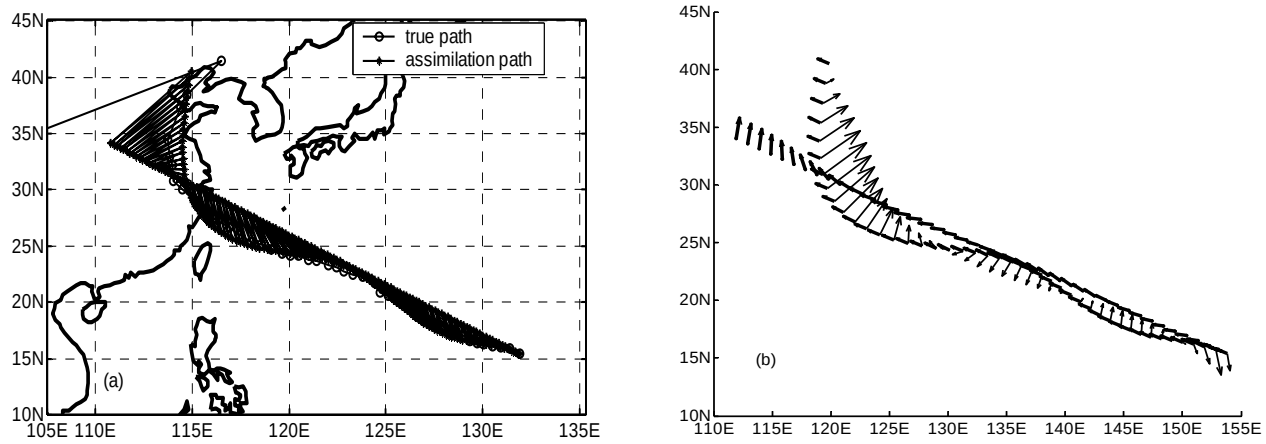

Fig. 9. TC Winnie with the track data every six hours. (a) The fitted and real track; (b) The retrieved velocity vector (bold, unit: (°) h^{-1}) and the resultant of the retrieved force and Coriolis force (light, unit: ×116.8 N) during the whole span of the TC motion.

data of TC 9804 as an example. The specific procedure is as follows: an assimilation of the data of the first 12 hour track is implemented, and then, the data of the succeeding 12 hour track is added to fulfill the same assimilation, and so on. The retrieved velocity and the resultant of the retrieved force and Coriolis force are shown in Fig. 7.

From Fig. 7, it can be seen that, in the period of the first 72 hours, the distribution of the retrieved velocity and the resultant of the retrieved force and Coriolis force is a little different from that of the complete TC track data shawn in Fig. 2b; however, from the first 84 hours on, with the increasing amount of TC track data used, the distribution of the retrieved velocity and the resultant of the retrieved force and Coriolis force is almost the same as that of the complete TC track data, which shows that the algorithm in this paper is stable when using a sufficient amount of TC track data.

4. Double-eyewalled TC cases

It is now accepted that the accuracy of TC track forecasts has been improved, although there are still a lot of problems remaining to be solved. So, the prevailing research focuses on the effects of changes in the complicated mesoscale structure of typhoons, such as the breaking and restoration of the eyewall, on the track and intensity of the typhoons.

A concentric double-eyewalled mesoscale structure is often observed in strong TCs both in the Northwest Pacific Ocean and in the Atlantic Ocean. Double eyewalls usually mean the pattern of inner and outer convective rings, with an inner ring diameter of 13 km

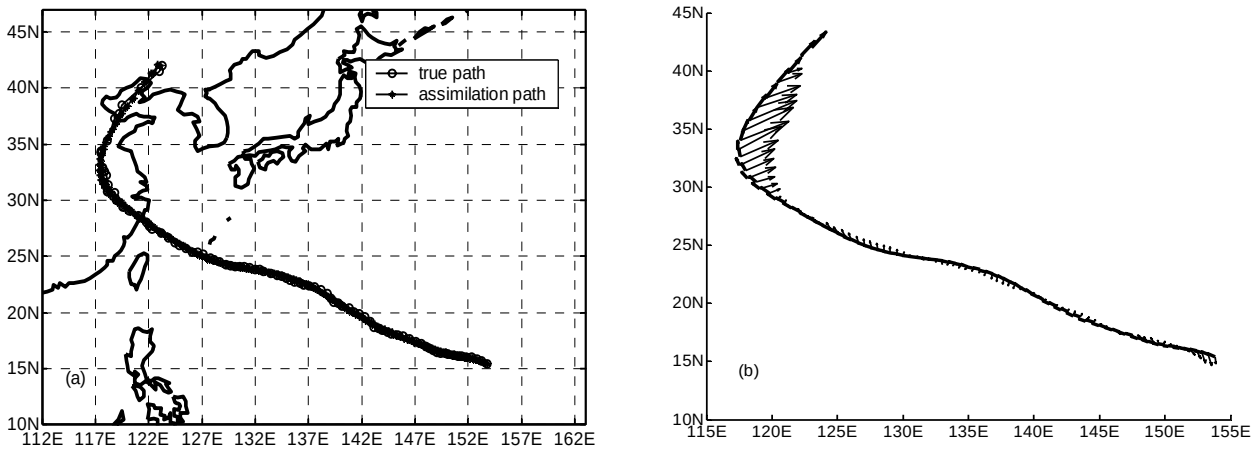

Fig. 10. TC Winnie with the track data every three hours. (a) The fitted and real track; (b) The retrieved velocity vector (bold, unit: $(^\circ)\,\mathrm{h}^{-1}$) and the resultant of the retrieved force and Coriolis force (light, unit: $\times 116.8$ N) during the whole span of the TC motion.

and an outer ring diameter of 46 km (Chen and Ding, 1979; Peng et al., 2004). Now, Zhu et al. (2004) modeled hurricane Bonnie (1998) using the Fifth-Generation Pennsylvania State University–National Center for Atmospheric Research Mesoscale Model (MM5). And both the simulated and observed storms also appeared to exhibit eyewall replacement scenarios in which the storms weaken as double eyewalls appear, and then reintensify as their inner eyewalls diminish and concentric eyewalls develop. Their results indicate that the eyewall replacement process may be predictable because it appears to depend on the large-scale flow. Here, we choose two double-eyewalled TCs occurring in the Northwest Pacific Ocean to check the applicability of the present method: Bilis (2000) and Winnie (1997).

The track data of TC Bilis was obtained every three hours.The fitted track and resultant of the retrieved force and Coriolis force are shown in Fig. 8, indicating that the present method can also be applied to the cases of double-eyewalled TCs.

Now we turn to TC Winnie. The track data of TC Winnie was mostly obtained every six hours. The fitted track and resultant of the retrieved force and Coriolis force are shown in Fig. 9. From the figure, it can be seen that the track is fitted badly. In checking the calculation process, it can be seen that the iteration algorithm stops at a large level of the cost functional, not at a small value. If interpolation procedure is performed (perhaps with some error) so that the track data of TC Winnie appear every three hours, then the track is fitted well, and the fitted track, retrieved velocity and resultant of the retrieved force and Coriolis force match well (Fig. 10).

Therefore, it can be concluded that the present method applies to TCs with evolving complicated mesoscale structures, such as double-eyewall structures and so on, provided that the temporal resolution of the track data is once every three hours.

5. Conclusions and discussion

In this paper, a variational data assimilation by the adjoint method is carried out for five real TC tracks, and the model used is the statistical-dynamical prediction model SD–90. The results indicate that, although the TC motions are very complicated, the TC tracks can be fitted well; for a given TC, the distribution of the resultant of retrieved force and Coriolis force well matches the corresponding TC track. That is, when a TC turns, the resultant of the retrieved force and Coriolis force acts as a centripetal force, which means that TCs behave like particles, which also verifies the validity of the point vortex viewpoint. Furthermore, the distribution of the resultants of retrieved forces and the Coriolis forces appears to be periodic in some cases. A variational data assimilation for a portion of the track of TC 9804 shows that the algorithm in this paper is stable when sufficient TC track data are used.

In all the turning tracks, recurvature accounts for a rather large percentage. Hodanish and Gray (1993), using data of North Pacific rawinsondes, investigated the interaction between the synoptic-scale circulation and tropical cyclones prior to, and during, the recurvature process, and their results show that the environmental wind fields at all levels of the troposphere are closely related to tropical cyclone motion prior to, and during, recurvature. For tropical cyclones that recurve, significant changes in the upper-tropospheric zonal wind fields were observed 1–2 days prior to beginning recurvature in the environmental sector northwest of the storm. Cyclones actually began to recurve

when positive zonal winds (westerlies) penetrated the middle and upper troposphere to within 6° of the cyclones' center. Tropical cyclones that did not recurve consistently showed negative zonal winds at this radius. Our results in this paper indicate that recurving is characterized by the resultants of the retrieved forces and the Coriolis forces as centripetal forces. Of course, the background corresponding to retrieved forces needs to be investigated further.

The SD–90 is now in use in operational TC prediction. Since the force $F_x(t)$ and $F_y(t)$ is determined according to the statistical regression method in SD-90, theoretically, the present method for determining $F_x(t)$ and $F_y(t)$ should be superior to the statistical regression method, as is shown above by the numerical results. For instance, TC turning is characterized by the resultant of the retrieved force and Coriolis force as a centripetal force. Therefore, theoretically, prediction of TC tracks based on the present method should have an advantage over that from SD–90. This is now under research and will be published in another paper.

Acknowledgments. Sincere appreciation is due to the two anonymous referees for their valuable suggestions. This work was supported jointly by the Typhoon Foundation of Shanghai, by LASG of the Institute of Atmospheric Physics of the Chinese Academy of Sciences, and by the National Natural Science Foundation of China under Grant No. 40633030.

REFERENCES

Chan, J. C. L., 2005: The physics of tropical cyclone motion. *Annual Review of Fluid Mechanics*, **37**, 99–128.

Chan, J. C. L, and R. T. Williams, 1987: Analytical and numerical studies of the beta-effect in tropical cyclone motion. Part I: Zero mean flow. *J. Atmos. Sci.* **44**, 1257–1265.

Chen Lianshou, and Ding Yihui, 1979: *The Western Pacific Typhoon Conspectus*. China Science Press, 491pp. (in Chinese)

Fiorino, M., and R. T. Elsberry, 1987: Some aspects of vortex structure related to tropical cyclone motion. *J. Atmos. Sci.*, **46**, 975–990.

Hodanish, Stephen, and William M. Gray, 1993: An observational analysis of tropical cyclone recurvature. *Mon. Wea. Rev.*, **121**, 2665–2689.

Huang Sixun, Han Wei, and Wu Rongsheng, 2004: Theoretical analyses and numerical experiments of variational assimilation for one-dimensional ocean temperature model with techniques in inverse problems. *Science in China* (D), **47**(7), 630–638.

Huang Sixun, and Wu Rongsheng, 2001: *Methods of Mathematical Physics in Atmospheric Science*. China Meteorologica Press, 540pp. (in Chinese)

Kuo, H. L., 1969: Motions of vortices and circulating cylinder in shear flow with friction. *J. Atmos. Sci.*, **26**, 390–398.

Li Tianming, and Zhu Yongti,1990: Analysis and modelling of tropical cyclone motions. I. The axisymmetric structure and the sudden change of tracks. *Science in China* (B), **34**, 104–112. (in Chinese)

Luo Zhexian, 1991: Possible causes of counterclockwise loop of tropical cyclones. *Science in China* (B), **35**, 769–775. (in Chinese)

Peng Jiayi, Fang Juan, and Wu Rongsheng, 2004: The formation mechanism of concentric double eyewall typhoon. Part I: Dynamical analysis. *Acta Meteorologica Sinica*, **18**, 301–312.

Smith, R. K., 1991: An analytic theory of tropical cyclone motion in a barotropic shear flow. *Quart. J. Roy. Meteor. Soc.*, **117**, 685–714.

Willoughby, H. E., 1992: Linear motion of a shallow-water barotropic vortex as an initial value problem. *J. Atmos. Sci.*, **49**, 2015–2031.

Wu, C. C., and Emanuel K. A., 1993: Interaction of a baroclinic vortex with background shear: Application to hurricane movement. *J. Atmos. Sci.*, **50**, 62–76.

Wu, L. G., and B. Wang, 2000: A potential vorticity tendency diagnostic approach for tropical cyclone motion. *Mon. Wea. Rev.,* **128**, 1899–911.

Xiang Jie, Wu Rongsheng, and Huang Sixun, 2004: Studies on application of the adjoint method to the statistic-dynamical prediction model for tropical cyclones (SD–90). I: Theoretical aspects and numerical tests. *Progress in Natural Sciences*, **14**, 677–682. (in Chinese)

Xiang Jie, and Wu Rongsheng, 2005:The effects of asymmetric wind structures of tropical cyclones on their tracks. *Acta Meteorologica Sinica*, **19**, 52–59.

Xue Zongyuan, and Li Zufeng, 1995: The statistic-dynamical prediction scheme for the tracks of tropical cyclones in the Northwest Pacific and the operational test results. *Atmospheric Science Research and Applications*, **5**, 59–65. (in Chinese)

Yeh, T. C., 1950: The motion of tropical storms under the influence of a superimposed southerly current. *Journal of Meteorlogy*, **7**, 108–113.

Zhu, T., D.-L. Zhang, and F. Weng, 2004: Numerical simulation of Hurricane Bonnie (1998). Part I: Eyewall evolution and intensity changes. *Mon. Wea. Rev.*, **132**, 225–241.